Journal of New Materials for Electrochemical Systems 19, 57-64 (2016)

Calcium Cobalt Hexacyanoferrate Cathodes for Rechargeable Divalent Ion Batteries

Prasanna Padigi, Neal Kuperman, Joseph Thiebes*, Gary Goncher, David Evans and Raj Solanki

Department of Physics, Portland State University, SRTC, 1719 SW 10th Ave, SB2-55, Portland, OR 97201, USA.

Received: March 15, 2016, Accepted: May 27, 2016, Available online: July 01, 2016

Abstract: *Calcium cobalt hexacyanoferrate (CaCoHCF) was synthesized and tested as a cathode material for rechargeable batteries, using divalent cations (Mg^{2+}, Ca^{2+}, Ba^{2+}). CaCoHCF demonstrated reversible specific capacity and coulombic efficiency (in parentheses) of 45.49 mAh/g (99.18%) for Mg^{2+}, 55.04 mAh/g (99.2%) for Ca^{2+}, and 44.09 mAh/g (99.42%) for Ba^{2+}, at a current density of 25 mA/g. Of the three ions, Ca^{2+} resulted in the highest absolute specific capacity as well as high specific capacity utilization. The cathodes were also subjected to rate capability measurements using current densities of 50 mA/g (30 cycles) and 0.1 A/g (100 cycles). Upon addition of 2 mL water to the non-aqueous electrolyte, the fraction of theoretical specific capacity increased to 55% for Mg^{2+}, 94.8% for Ca^{2+}, and 95.53% forBa^{2+}. This increase has been interpreted as the ability of the cathode material to intercalate and de-intercalate more ions due to the electrostatic shielding provided by water molecules between the host lattice and the guest cations. An empirical relationship between the cation size and specific capacity utilization is presented.*

Keywords: multivalent ion; calcium cobalt hexacyanoferrate; intercalation; rechargeable battery

1. INTRODUCTION

With the increasing prevalence of portable electronics, electric vehicles, and intermittent sources of renewable energy, comes greater demand for high energy density rechargeable batteries. At present, most commercial rechargeable batteries utilize the Li^+ ion as a charge carrier, with cathodes composed of lithium-doped metal oxides [1]. While lithium has proved very useful, its limitations make other charge carriers and electrode materials appealing. In particular, the toxicity of lithium along with its flammability creates engineering challenges for safe electrochemical cells [2]. Moreover, the limited abundance of lithium in the earth's crust leads to ever-increasing costs associated with mining lithium [3].

In principle if abundant, non-toxic ions and materials can be used in energy storage, associated costs may be reduced significantly. Iron hexacyanoferrate (also known as the pigment Prussian blue) has been investigated as an intercalation cathode that can accommodate a variety of ions due to its relatively large lattice spacing and cubic structure [4]. Because of these properties, larger multivalent ions can be used, which carry more charge than monovalent ions and therefore could lead to high volumetric energy density batteries. We have therefore examined calcium cobalt hexacyanoferrate, a Prussian blue analog,as a cathode material for multivalent ions. This material,which was composed of 15-20 nm crystallites, served as a host for intercalation of Ca^{2+}, Ba^{2+}, and Mg^{2+} ions.

Another important consideration when using multivalent cations is their high polarizing power that results in strong electrostatic interaction with the host lattice that can limit intercalation [5-9]. This can be remedied by adding a small quantity of water, which shields the multivalent ions by forming a hydration sphere around them in the organic electrolyte. This reduces the coulombic interactions with the host material, so that intercalation can occurwith less internal resistance.

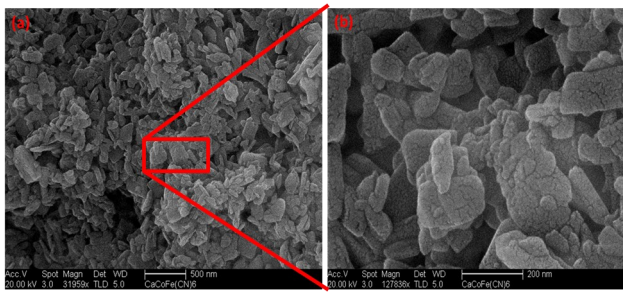

Figure 1. Scanning electron micrographs of $CaCoFe(CN)_6$ synthesized at 60°C (a) with a scale bar of 500 nm. (b) Expanded inset showing $CaCoFe(CN)_6$ with a scale bar of 200 nm.

*To whom correspondence should be addressed: Email: jthiebes@pdx.edu
Phone:

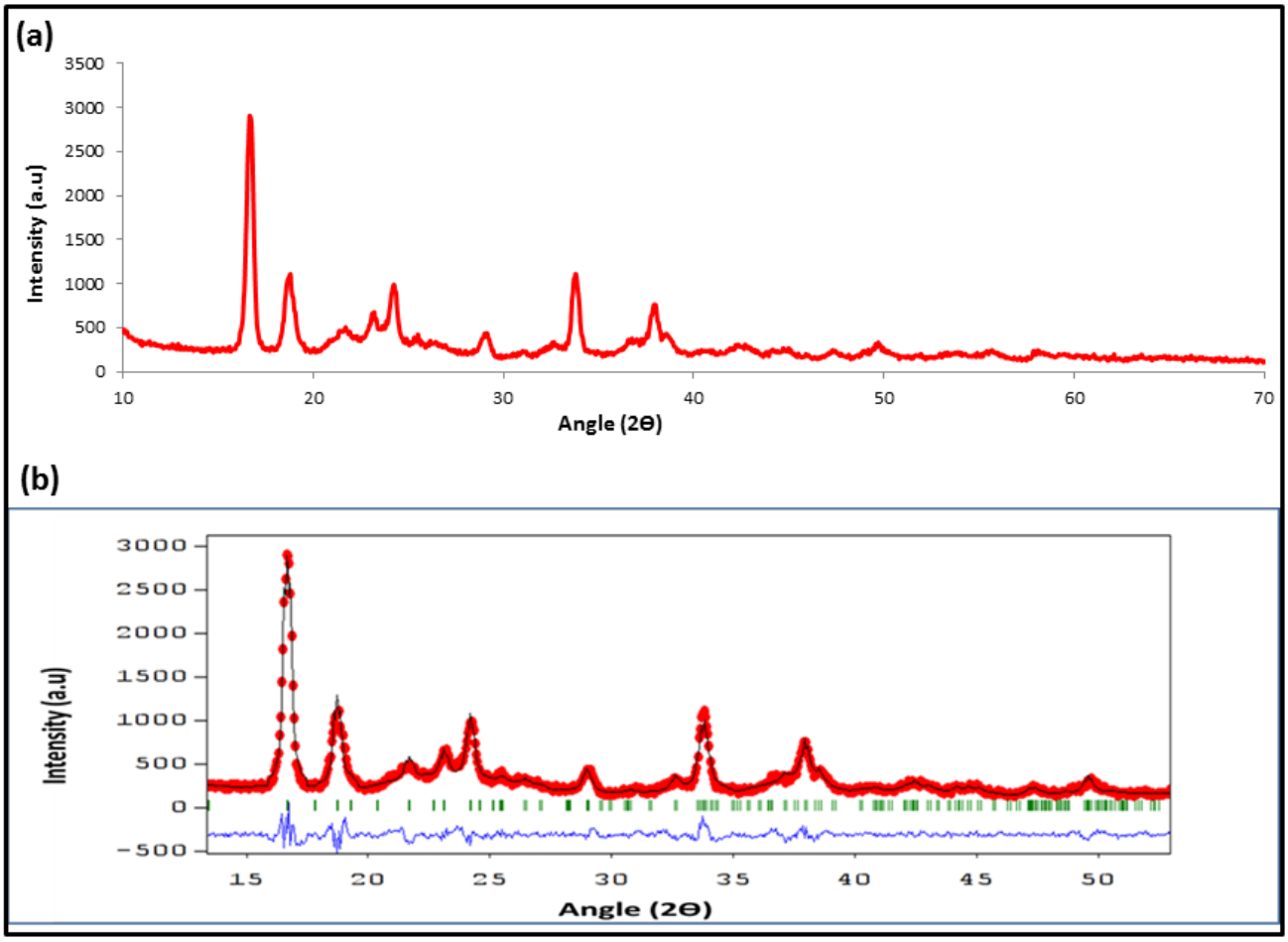

Figure 2. (a). Raw powder XRD pattern of the as synthesized $CaCoFe(CN)_6$, (b).Rietveld refined powder XRD pattern of the as-synthesized $CaCoFe(CN)_6$ (solid line) with superimposed raw data (dotted line).

We report the performance of calcium cobalt hexacyanoferrate as an intercalation cathode material in an electrochemical cell, utilizing Ca^{2+}, Ba^{2+}, and Mg^{2+} ions, and also show that it does not have the same cubic structure as Prussian blue. Further, it is demonstrated that addition of a small quantity of water to the organic electrolyte solution improves performance as expected from previous results[5-9].

2. EXPERIMENTAL SECTION

2.1. Synthesis

5 mmoles of calcium ferrocyanide ($Ca_2Fe(CN)_612H_2O$) were dissolved in 25 ml de-ionized (DI) water and heated to 60°C on a hot plate under magnetic stirring. 2.5 mmoles of cobalt chloride hexahydrate ($CoCl_26H_2O$) were dissolved in 25 ml DI water under magnetic stirring. Cobalt chloride solution was added in a drop-wise manner to the solution of calcium ferrocyanide under magnetic stirring at 60°C, resulting in the precipitation of calcium cobalt hexacyanoferrate, $CaCoFe(CN)_6$. The solution with the precipitate was maintained at 60°C for 2 hours under constant magnetic stirring. The precipitates were cleaned with DI water using centrifuga-

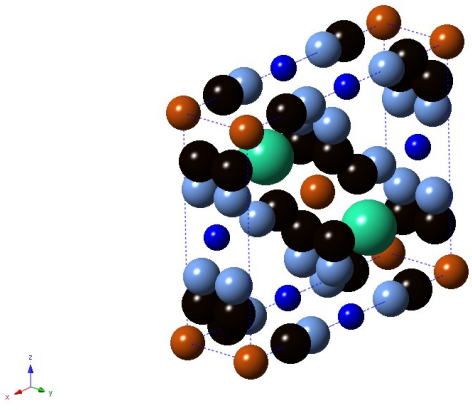

Figure 3. Schematic of unit cell of $CaCoFe(CN)_6$. The Fe^{2+} ions are represented by red spheres. The CN^- bridging ligand is represented by black and light blue spheres. Co^{2+} ions are represented by indigo blue spheres. The interstitial Ca^{2+} ions are represented by large green spheres.

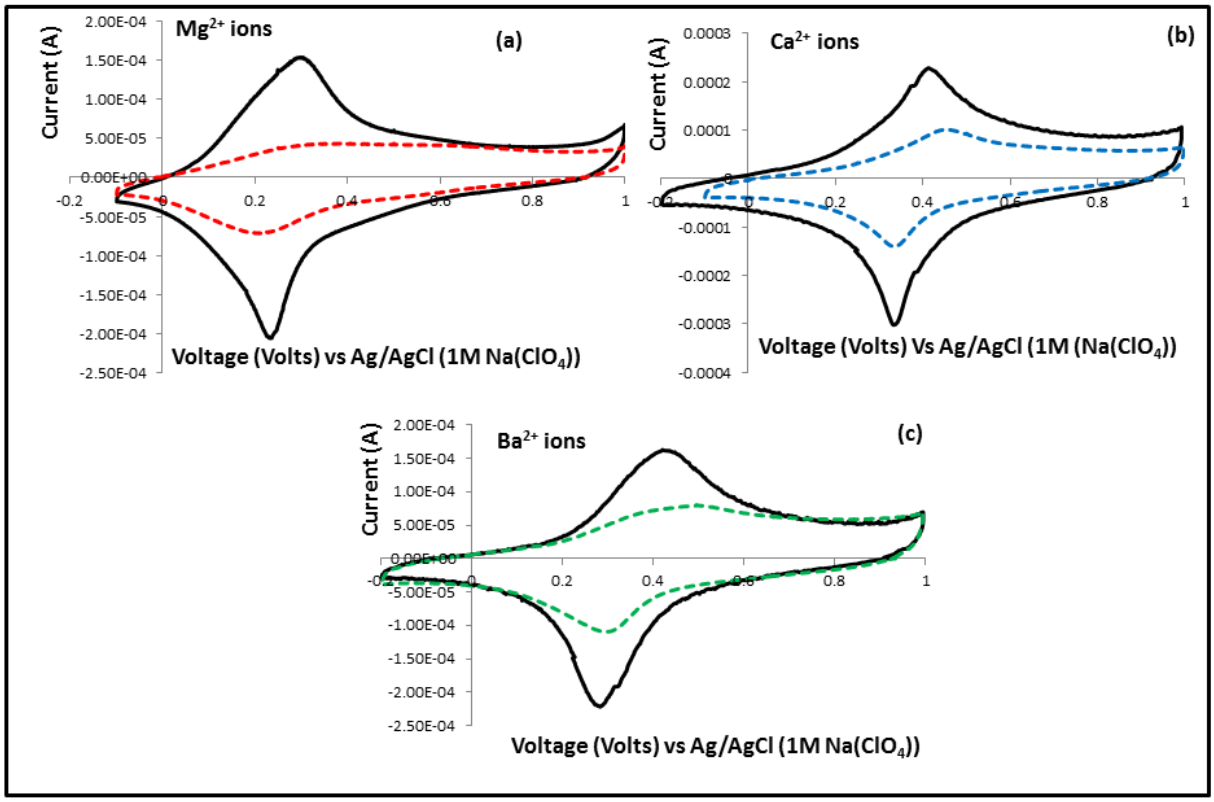

Figure 4. Cyclic voltammograms (CV) of calcium cobalt hexacyanoferrate in 1M $Ca(ClO_4)_2$, 1M $Mg(ClO_4)_2$, and 1M $Ba(ClO_4)_2$in acetonitrile with a scan rate of 0.5 mV/sec. The dashed lines represent the measurements in stock solutions and the solid black lines represent the measurements after adding 2 ml of DI water to the respective stock solutions.

tion at 7,000 rpm and dried in air, resulting in bright green colored calcium cobalt hexacyanoferrate powders. The ferrocyanide to cobalt ion ratio of 2:1 was chosen, as previously reported in the literature [2], to achieve redox activity in cobalt in the synthesized structure.

2.2. Physical Characterization: Scanning Electron Microscopy

The as-synthesized calcium cobalt hexacyanoferrate (CaCoHCF) powders were analyzed using scanning electron microscopy (SEM) using a secondary electron detector to determine the morphology and size distribution of the particles. Figure 1(a) and 1(b) show the SEM images of $CaCoFe(CN)_6$ synthesized at 60°C with the Co^{2+}:$Fe(CN)_6^{4-}$ ratio of 1:2. The images indicate a porous platelet-like morphology with a thickness in the range of 30-50 nm. Each of the platelets was composed of nanoparticles with the sizes in the range of 15-25 nm. The $CaCoFe(CN)_6$ powders were imaged using a 20 kV beam.

2.3. Physical Characterization: Powder X-ray Diffraction (PXRD)

The phase composition of the $CaCoFe(CN)_6$ sample (60°C) was characterized using powder X-ray diffractometry (PXRD) on a Rigaku Ultima IV x-ray diffraction system (Rigaku Americas, The Woodlands, TX). Scans were performed over a 2θ range of 10°–70° at room temperature. The PXRD spectrum is shown in Figure 2.The dominant peaks occur at 16.7°, 18.70°, 21.40°, 23.10°, 24.20°, 25.0°, 28.90°, 30.5°, 32.2°, 33.7° and 37.9°. It is evident from the shape of the peaks that the as-formed $CaCoFe(CN)_6$ possessed good crystallinity, as indicated by the well-defined symmetry.

The XRD spectrum was analyzed by Rietveld analysis using the XRD peak indexing software DicVol under the FULLPROF [10] suite, as shown in Figure 2. This information was used to identify the unit cell lattice symmetry as monoclinic belonging to the P 2/m space group, with the unit cell parameters determined to be as follows: a_0 = 10.76778Å, b_0 =3.92032 Å and c_0 = 9.59701 Å and α=γ=90°, β=98.91652°. A unit cell fitting these parameters is shown in Figure 3.

2.4. Cathode Preparation and Electrochemistry set-up

The cathode electrode was prepared by mixing $CaCoFe(CN)_6$ powder with multi-walled carbon nanotubes, carbon black and polyvinylidene fluoride (PVDF) binder in a ratio of 80:9:2:9 and was then groundfinely using a mortar and pestle. Aslurry was prepared by adding a few drops of N-methyl-2-pyrolidone (NMP) to the above formed homogeneous powder and spread on both sides

of a carbon fiber paper which acted as the current collector. The slurry-coated electrodes were initially dried at room temperature and further dried under vacuum at 100°C for 2 hours.

The electrochemical performance of $CaCoFe(CN)_6$ was evaluated using cyclic voltammetry and galvanic cyclingat ambient temperature. The test cell was comprised of a glass container with three electrodes, where a graphite rod acted as a counter electrode, carbon paper coated with $CaCoFe(CN)_6$ was the working electrode, and a Ag/AgCl(1M $Na(ClO_4)$) filled capillary tube was the reference electrode. All the measurements were made with 2 $cm^2$of the working electrode exposed to the electrolyte solution. The stock electrolyte for all measurements was composed of 1M $Ca(ClO_4)_2 3.5H_2O$for Ca^{2+} ions, 1M $Mg(ClO_4)_2 6H_2O$ forMg^{2+} ions, and 1M $Ba(ClO_4)_2 3H_2O$ for Ba^{2+} ions in acetonitrile as the organic solvent. Initial measurements were performed using the stock electrolyte. Subsequently 2 ml of water were added to the electrolyte solutions as described below. In the present work, charging is represented by de-intercalation (or removal) of metal ions, M'(M'= Mg^{2+}, Ca^{2+}, Ba^{2+}) and discharging by intercalation (insertion) of metal ions, into the $CaCoFe(CN)_6$ electrode, which is used as a cathode. The reaction mechanisms with Ca ions can be summarizedas:

$$CaCoFe^{(II)}(CN)_6 \longrightarrow Ca_{0.5}CoFe^{(III)}(CN)_6 + 0.5Ca^{2+} + e^- \quad \text{(first charge cycle)} \quad (1)$$

$$Ca_{0.5}CoFe^{(III)}(CN)_6 + 0.5\ Ca^{2+} + e^- \text{ (charging)} \longleftrightarrow CaCoFe^{(II)}(CN)_6 \text{ (discharging)} \quad (2)$$

Equation (1) represents the reaction of the first charge cycle and equation (2) the reaction for the subsequent discharge and charge cycles. For charge-discharge measurements, the electrodes were subjected to the following current densities: 25 mA/g (30 cycles), 50 mA/g (30 cycles) and 100 mA/g (100 cycles), with an upper cut-off voltage of 0.8 V and a lower cut-off voltage of 0 Vwith respect to Ag/AgCl (1M $Na(ClO_4)$).

3. RESULTS AND DISCUSSION

3.1. Electrochemical Characterization: Cyclic Voltammetry (CV)

The CaCoHCF cathodes were subjected to electrochemical characterization to confirm redox processes and to identify the redox potentials. The experimental set up used to perform cyclic voltammetry with Ca^{2+} ions, Mg^{2+} ions, and Ba^{2+} ions is described in Section 2.4. The voltage on the CaCoHCF cathodes were scanned with respect to the Ag/AgCl reference electrode and current was measured between the CaCoHCF working electrode and the carbon counter electrode.

Figure 4 shows the cyclic voltammetry curves for CaCoHCF electrode using Mg^{2+} ions, Ca^{2+} ions, and Ba^{2+} ions using their respective stock solutions at a scan rate of 0.5 mV/sec. The cyclic voltammetry measurements showed a single oxidation peak and a single reduction peak for all three ions. The dashed lines represent the CV measurements in stock solutions for the respective ions. The CV curves in solid black line represent the measurements made in stock solutions after adding 2 ml of DI water to them.

a) Mg^{2+} ions: The CaCoHCFcathode demonstrated reversible single step insertion (0.221 V) and extraction (0.319 V) of Mg^{2+} ions, as shown in Figure 4(a), resulting in a peak voltage separation of 0.098V and a peak oxidation current to peak reduction current ratio of 0.59.

Upon addition of 2 ml water, the cathode demonstrated reversible single step insertion (0.283 V) and extraction (0.246 V) of Mg^{2+} ions, as shown in Figure 4(a), resulting in a peak voltage separation of 0.037 V and a peak oxidation current to peak reduction current ratio of 0.76.

b) Ca^{2+} ions: The CaCoHCF cathode demonstrated reversible single step insertion (0.355 V) and extraction (0.433 V) of Ca^{2+} ions similar to Mg^{2+} ions, as shown in Figure 4(b), resulting in a peak voltage separation of 0.078 V and a peak oxidation current to peak reduction current ratio of 0.75. Upon addition of 2 ml water, the cathode demonstrated reversible single step insertion (0.345 V) and extraction (0.398 V) of Ca^{2+} ions, as shown in Figure 4(b), resulting in a peak voltage separation of 0.05 V and a peak oxidation current to peak reduction current ratio of 0.76.

c) Ba^{2+} ions: The CaCoHCF cathode demonstrated reversible single step insertion (0.31 V) and extraction (0.483 V) of Ba^{2+} ions similar to $Mg^{2+}$and Ca^{2+}ions, as shown in Figure 4(c), resulting in a peak voltage separation of 0.173 V and a peak oxidation current to peak reduction current ratio of 0.73. Upon addition of 2 ml water, the cathode demonstrated reversible single step insertion (0.296 V) and extraction (0.42 V) of Ba^{2+} ions, as shown in Figure 4(c), resulting in a peak voltage separation of 0.124 V and a peak oxidation current to peak reduction current ratio of 0.77.

The CV measurements with water indicate a significant increase in peak oxidation and peak reduction currents, as well as more defined oxidation and reduction peaks for all three ions. The rises in peak definition when water was added to the solutions indicate faster kinetics associated with the insertion and extraction of ions into the host lattice. This has been attributed to the presence of a hydration sheath around the intercalating guest ions, resulting in reduced electrostatic interactions between the host CoHCF lattice

Table 1. Summary of results of the CV measurements using CaCoHCF cathode with the three ions (Mg^{2+}, Ca^{2+} and Ba^{2+}).

Ion (M')	Peak oxidation Potential (V)	Peak reduction potential (V)	Peak voltage difference (ΔV)	I_{ox}/I_{red}
Mg^{2+}	0.319	0.221	0.098	0.59
Ca^{2+}	0.433	0.355	0.078	0.75
Ba^{2+}	0.483	0.31	0.173	0.73
Mg^{2+}/2ml water	0.283	0.246	0.037	0.76
Ca^{2+}/2ml water	0.397	0.347	0.05	0.76
Ba^{2+}/2ml water	0.42	0.296	0.124	0.77

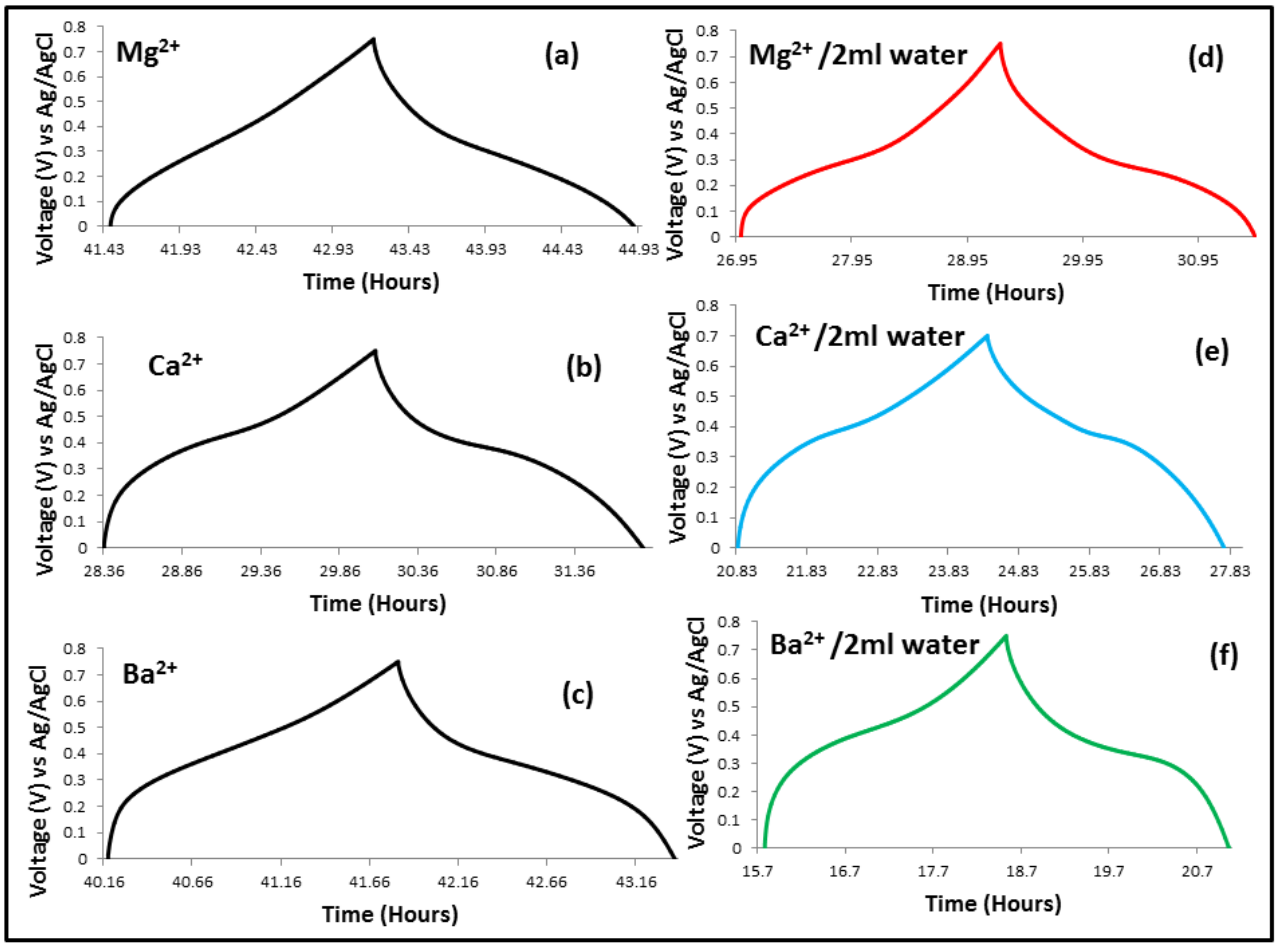

Figure 5. Charge-discharge profiles of calcium cobalt hexacyanoferrate at a current density of 25 mA/g using (a) 1M $Mg(ClO_4)_2 6H_2O$ in acetonitrile, (b) 1M $Ca(ClO_4)_2$ $3.5H_2O$ in acetonitrile, (c) 1M $Ba(ClO_4)_2 3H_2O$ in acetonitrile, (d) 1M $Mg(ClO_4)_2 6H_2O$ in acetonitrile and 2ml DI water, (e) 1M $Ca(ClO_4)_2 6H_2O$ in acetonitrile and 2ml DI water, (f) 1M $Ba(ClO_4)_2 6H_2O$ in acetonitrile and 2ml DI water.

and the guest intercalating ions [3]. The lower peak voltage separation (ΔV), and the ratio of peak oxidation current and peak reduction current (I_{ox}/I_{red}) being closer to 1, indicates that the addition of water to the electrolyte increased the reversibility associated with the insertion and extraction of all three divalent ions from the CoHCF lattice. The CV measurement data for all three ions have been summarized in Table 1. The addition of water to the electrolyte was observed to reduce the peak oxidation and peak reduction voltages, due to a reduction in the activation energy for insertion and extraction of the divalent ions from the host lattice [4].

3.2. Electrochemical Characterization:Galvanic Cycling (GC)

The CaCoHCF cathode was subjected to galvanic cycling, which involved charging and discharging the cathode, by applying a constant current and measuring the cathode voltage against Ag/AgCl (1M $NaClO_4$) reference electrode with respect to time. An upper cut-off voltage of 0.8V and a lower cut-off voltage of 0V were defined to mark the limits of charging and discharging processes. Figures5(a-c) show charge-discharge curves of the CaCoHCF cathode with a constant current density of 25 mA/g with each of Mg^{2+},Ca^{2+}, Ba^{2+}in their respective stock solutions. Their corresponding charge-discharge curves after adding 2 ml of DI water are shown in Figure 5(d-f).

Reversible specific capacity and coulombic efficiencyof the CaCoHCF cathodes were determined based on the amount of time required to reach the upper cut-off voltage for charging and lower cut-off voltage for discharging, the mass of the active cathode material, and the applied current. The reversible specific capacity and coulombic efficiency (in parenthesis) were 48.57 mAh/g (99.18%), 55.04 mAh/g (99.2%) and 44.09 mAh/g (99.42%) for Mg^{2+}, Ca^{2+} and Ba^{2+} ions, respectively, at a current density of 25 mA/g over 30 cycles of charging and dischargingas shown in Figures 6(a, c, e).This resulted in a capacity utilization of 47.82%, 63.60% and 66.89% when compared to the calculated theoretical specific capacity of 95.12 mAh/g, 86.53 mAh/g and 65.91 mAh/g for Mg^{2+}, Ca^{2+} and Ba^{2+} ions, respectively.

To study the effect of increasing current density on the specific capacity, the CaCoHCF cathodes were subjected to galvanic cycling at two additional current densities of 50 mA/g over 30 cycles

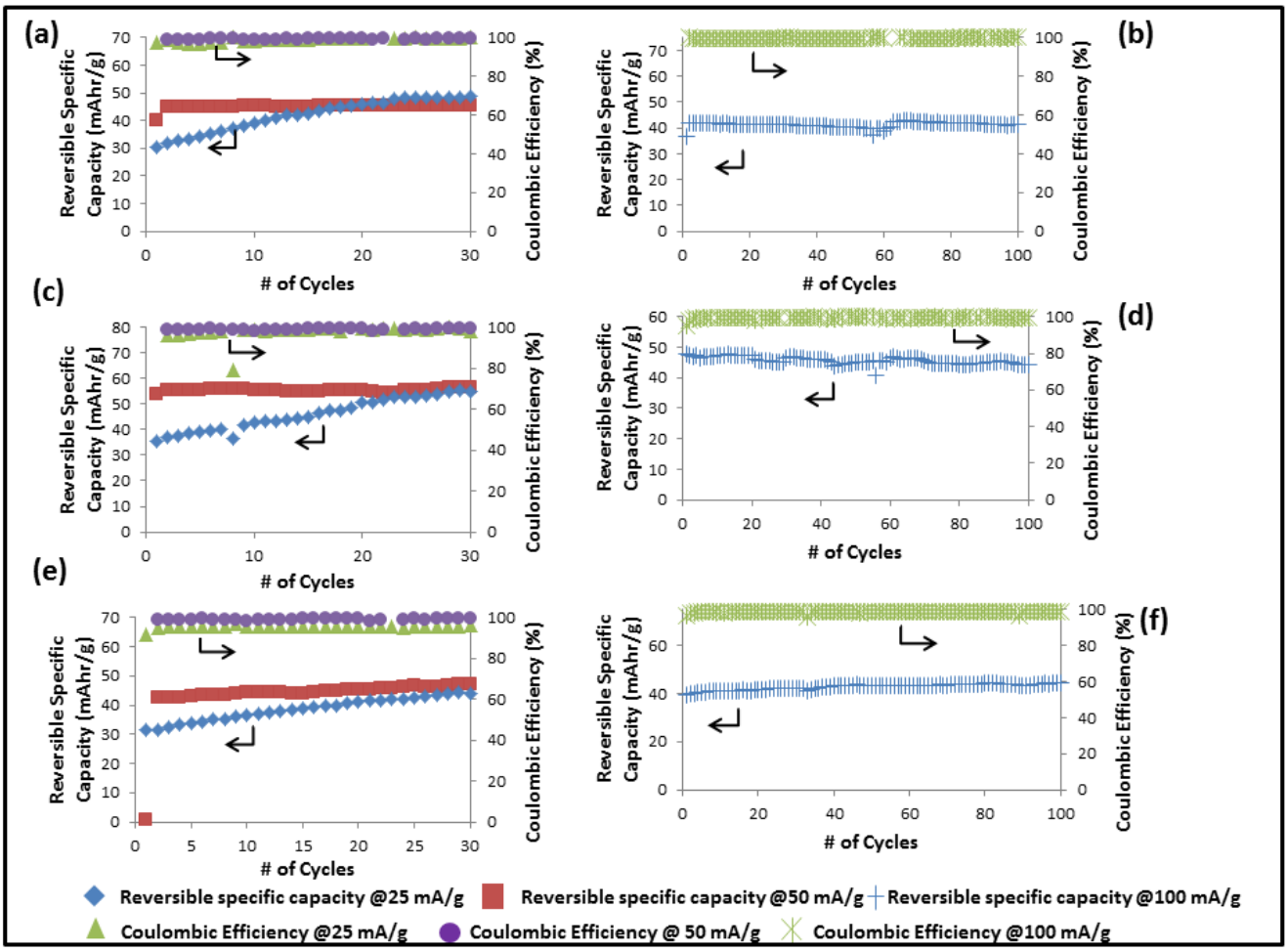

Figure 6. Reversible specific capacity and coulombic efficiency versus number of cycles for CaCoHCF electrode at the following current densities: 25 mA/g, 50 mA/g and 100 mA/g for: (a, b) Mg^{2+} ions, (c, d) Ca^{2+} ions and (e, f) Ba^{2+} ions.

and 100 mA/g over 100 cycles. At the 50mA/g current density, the reversible specific capacity and coulombic efficiency (in parentheses) for Mg^{2+}, Ca^{2+} and Ba^{2+} ions were:48.57 mAh/g(99.34%), 56.6 mAh/g (99.4%) and 46.97mAhr/g (99.34%), respectively. For the 100 mA/g current density, the respective reversible specific capacity and coulombic efficiency (in parentheses) were: 41.06 mAh/g (99.9%), 44.22 mAh/g (99.7%) and 44.13mAhr/g (98.6%). The minimal loss in reversible specific capacities and very high coulombic efficiencies at higher current densities for the three ions suggests that the CaCoHCF cathodes possess excellent rate capability and reversibility, in terms of their ability to store charge over the above mentioned number of cycles, as shown in Figures 6 (a-f). The rate capability measurements have been summarized in Table 2.

In order to study the performance of CaCoHCF cathodes for the above-mentioned ions in a mixed solvent environment, 2 ml DI water was added to the stock electrolyte solutions for all three ions and subjected to galvanic cycling at a current density of 25 mA/g.

Table 2. Summary of rate capability measurements using CaCoHCF cathodes with Mg^{2+}, Ca^{2+} and Ba^{2+} ions.

Ion (M')	Theoretical Specific Capacity (mAh/g)	Reversible Specific Capacity at 25 mA/g (mAh/g)	Reversible Specific Capacity at 50 mA/g (mAh/g)	Reversible Specific Capacity at 100 mA/g (mAh/g)
Mg^{2+}	95.12	45.49	48.57	41.06
Ca^{2+}	86.5	55.04	56.6	44.22
Ba^{2+}	65.91	44.09	46.97	44.13
Mg^{2+}/2ml water	95.12	52.83	47.48	39.75
Ca^{2+}/2ml water	86.5	82	70.85	55.95
Ba^{2+}/2ml water	65.91	62.97	58.56	52.1

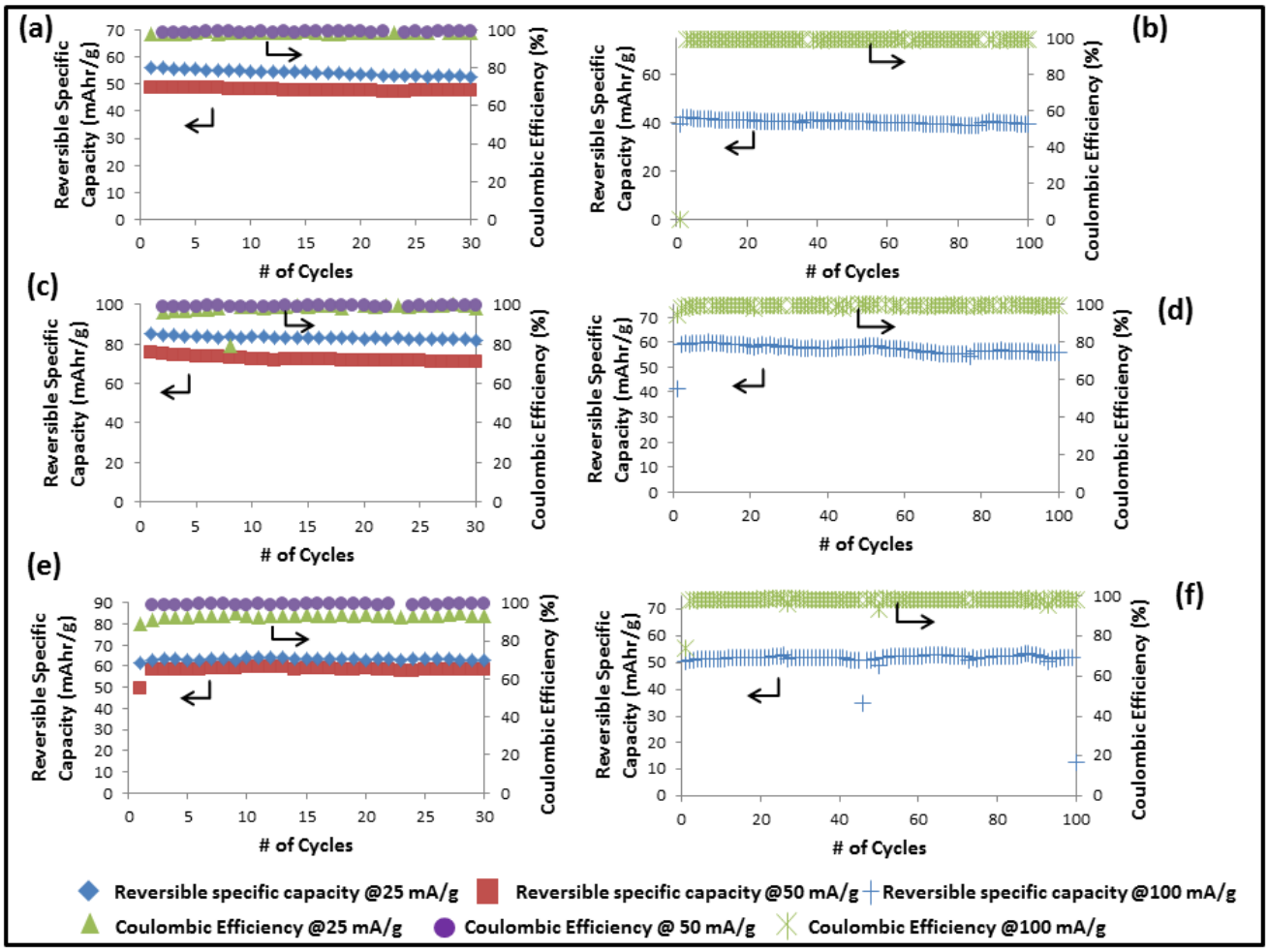

Figure 7. Reversible specific capacity and coulombic efficiency versus number of cycles for CaCoHCF electrode with 2 ml water added to the stock electrolyte, at the following current densities: 25 mA/g, 50 mA/g and 100 mA/g for: (a, b) Mg^{2+} ions, (c, d) Ca^{2+} ions and (e, f) Ba^{2+} ions.

This resulted in the following reversible specific capacities and (coulombic efficiencies) for Mg^{2+}, Ca^{2+} and Ba^{2+} ions, respectively: 52.83 mAh/g (98.6%), 82 mAh/g (96.3%) and 62.97 mAh/g (92.8%), as shown in Figures 7(a, c, e). The specific capacities translated into a capacity utilization of 55.54%, 94.8% and 95.53% for Mg^{2+} ions, Ca^{2+} ions and Ba^{2+} ions, respectively. This amounted to an increase in specific capacity utilization by 7.7% for Mg^{2+} ions, 31.17% for Ca^{2+} ions and 28.63% for Ba^{2+} ions when compared against the values measured with the stock solutions alone as the electrolytes.To study the effect of increasing current density on the specific capacity, the CaCoHCF cathodeswere further subjected to galvanic cycling at two additional current densities of 50 mA/g over 30 cycles and 100 mA/g over 100 cycles using Mg^{2+}, Ca^{2+} and Ba^{2+} ions, as shown in Figures 7 (a-f). The results for the rate capability measurement with water have been summarized in Table 2.

As stated previously, the increase in reversible specific capacity utilization for all three cations, upon addition of DI water, is postulated to result from the presence of a hydration sheath around the guest cations. The hydration sheath provides additional electrostatic shielding between the positive charge possessed by the cations and the net negative charged host lattice. This allows for enhanced diffusion of the guest species into the interstitial spaces of the host lattice and access to the redox sites, thereby, increasing the gravimetric capacity utilization [5-9].

From the data in Table 2 it can be observed that the specific capacity utilization increases from the smallest ion (Mg^{2+}) to the largest ion (Ba^{2+}) in the series. Since all these ions are doubly charged, the smallest ion (Mg^{2+}) should interact most strongly with the hexacyanoferrate lattice. Investigations of the bonding between ions have shown a direct correlation between the quantity z/r^2 and polarizing power of the ions [11,12], where z is the charge on the ions and r is the ionic radius. In Figure 8 we have plotted the specific capacity utilization for several intercalating ions in CoHCF vs. the polarizing power $z/r^2$of the ions. The radius used for calculation is the effective ionic radius for a coordination number of 8 [13]; radii used for Mg^{2+}, Ca^{2+} and Ba^{2+} ions were 89 pm, 112 pm, and 142 pm respectively. There is a good linear fit to the data (c^2 = 0.0006216), indicating a good correlation between polarizing pow-

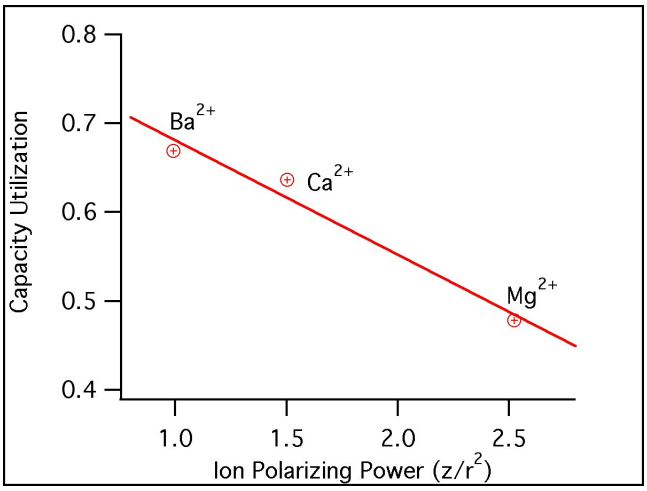

Figure 8. Specific capacity utilization versus polarizing power of guest cations.

er of the intercalating ion and the capacity of the cell. We interpret these results to mean that ions with lower polarizing power, that interact less strongly with the lattice, are able to intercalate into the lattice better, resulting in higher capacity.

Although from this data Ba^{2+} ions had the highest specific capacity utilization (capacity as a percent of maximum theoretical capacity), the highest specific capacity was observed for Ca^{2+}ions in CoHCF. Overall, the best combination of specific capacity and capacity utilization was observed with Ca^{2+} as the doubly charged intercalating ion.

4. CONCLUSION

$CaCoFe(CN)_6$ was synthesized and tested as a cathode material for Mg^{2+}, Ca^{2+}, and Ba^{2+} divalent ions, using acetonitrile as an organic solvent and acetonitrile with 2 ml water as a mixed solvent for the electrolytes. The hydration sheath due to the addition of water to acetonitrile was observed to increase the specific capacity utilization for all the three ions, due to the electrostatic shielding provided by the sheath. It was also observed that the decrease in the polarization power of the guest cation resulted in an increase in the specific capacity utilization of the CaCoHCF cathode, due to decreased electrostatic interactions between the guest cation and the host CoHCF lattice. Among the tested ions, the use of Ca^{2+} ions as the guest species resulted in highest absolute specific capacity as well as high specific capacity utilization.

5. ACKNOWLEDGEMENTS

We would like to thank Arkema for providing us with HSV900PVDF binder. We would also like thank Dr.Goforth for allowing access to the XRD system (NSF-MRI, Award No. DMR-0923572) and Sheng Kuei Chiu for helping us with the XRD measurements.

REFERENCES

[1] Liu, J.; Xia, H.; Xue, D.; Lu, L., J. Am.Chem. Soc., 131(34), 12086 (2009).

[2] Kim, H.; Jeong, G.; Kim, Y.U.; Kim, J.H.; Park, C.M.; Sohn, H.J., Chem. Soc. Rev., 42(33), 9011 (2013).

[3] Yoo, H. D.; Shterenberg, I.; Gofer, Y.; Gershinsky, G.; Pour, N.; Aurbach, D., Energy Environ. Sci., 6(8), 2265 (2013).

[4] Padigi, P.; Thiebes, J.; Swan, M.; Goncher, G.; Evans, D.; Solanki, R. Prussian Green, Electrochim. Acta, 166, 32 (2015).

[5] Padigi, P.; Goncher, G.; Evans, D.; Solanki, R.;, J. Power Sources, 273, 460 (2015).

[6] Levi, E.; Gofer, Y.; Aurbach, D., Chem. Mater., 22(3), 860 (2009).

[7] Novak, P.; Scheifele, W.; Haas, O., J. Power Sources, 54, 479 (1995).

[8] Crumbliss, A. L.; Lugg, P. S.; Morosoff, N., Inorg. Chem., 23, 4701 (1984).

[9] Novak, P.; Disilvestro, J., J. Electrochem. Soc., 140, 140 (1993).

[10]Rodríguez-Carvajal, J. "FULLPROF: A Program for Rietveld Refinement and Pattern Matching Analysis." Abstracts of the Satellite Meeting on Powder Diffraction of the XV Congress of the IUCr, Toulouse, France. 1990, 127.

[11]Bertran, J.F.; Reguera-Ruiz, E.; and Pascual, J.B., Spectrochim. Acta, 46A, 1679 (1990).

[12]El Shafei, G.M.S., J. Colloid Interface Sci., 182, 249 (1996).

[13]Shannon, R.D., Acta Crystallogr., Sect. A: Found Crysallogr., 32, 751 (1976).